

# Nonuniversal transmission phases through a quantum dot: An exact-diagonalization of the many-body transport problem

Leslie O. Baksmaty, Constantine Yannouleas, and Uzi Landman  
*School of Physics, Georgia Institute of Technology, Atlanta, Georgia 30332-0430*  
(Dated: 24 January 2008)

Systematic trends of nonuniversal behavior of electron transmission phases through a quantum dot, with no phase lapse for the transition  $N = 1 \rightarrow N = 2$  and a lapse of  $\pi$  for the  $N = 2 \rightarrow N = 3$  transition, are predicted, in agreement with experiments, from many-body transport calculations involving exact diagonalization of the dot Hamiltonian. The results favor dot shape anisotropy and strong  $e - e$  repulsion with consequent electron localization, showing dependence on spin configurations and the participation of excited doorway transmission channels.

PACS numbers: 73.23.Hk, 73.21.La, 31.15.-p

*Motivation.* By enabling the measurement of transmission phases in addition to conductances, Aharonov-Bohm interferometry has provided a valuable experimental tool for obtaining information about fundamental transport properties through small systems [1, 2]. An experimental setup conceived and employed in such studies consists of placing a two-dimensional quantum dot (QD) in one of the arms of the two-path interferometer [1, 2]. In earlier experiments [1] a universal behavior of the phase was found where for each added electron the phase drops discontinuously by  $\pi$  (phase lapse, PL) before rising back (as expected) continuously by the same amount. This behavior was found to be independent of the number of electrons, the dot shape and spin degeneracy. The regime of mesoscopic (nonuniversal) behavior of the transport through the dot, exhibiting an irregular PL pattern and dependencies on the number of electrons and dot parameters has been observed only recently [2] for dots with a smaller number of electrons  $N < 15$ .

The large majority of theoretical studies attempted to address the PL behavior in the universal regime. Nevertheless, this behavior remains puzzling [3]. This state of affairs and the new issues brought about by the recent discovery of the nonuniversal regime motivated considerations of quantum fluctuations (i.e., going beyond the mean-field treatments) for investigation of the crossover from the mesoscopic to the universal regime [4].

In this paper, we focus on the nonuniversal regime (in the limit of a very small number of electrons) where as stated in Ref. [2] “the phase behavior for electron transmission should in principle be easier to interpret.” To this aim, we develop a transport theory based on a computational many-body microscopic theory, entailing exact diagonalization (EXD) [5] of the QD many-body Hamiltonian. This approach includes electron correlation effects and allows systematic investigations of the transport characteristics as a function of the dot shape, number of electrons, and spin configurations. In evaluating the transport properties, we follow the work of Bardeen [6] where the many-body states of the QD play a determining role (see below) [7]. The present electron-

transmission formalism has many analogies with that used in independent-particle approaches [8, 9], but with the crucial difference that many-body correlated *quasi-particles* [see Eq. (1)] are used for the dot states, instead of the simple single-particle orbitals of a central-mean-field-type confining potential.

In the mesoscopic regime ( $N < 15$ ) exhibiting nonuniversal characteristics, it is desirable to have precise knowledge about the dot parameters (e.g., shape and strength of interelectron repulsion). While such information is not available directly from the current experiments [2], we inquire here about systematic trends that appear in the calculations as a function of the dot parameters, with subsequent comparisons with the available data. The two key parameters that we vary in our study are: (a) the dielectric constant  $\kappa$ ; in order to drive the QD towards the regime of strong correlations, since the experimental QDs of Ref. [2] are shallower than usual, and (b) the anisotropy of the QD, since the sideways located plunger influences greatly the average confinement for small dots [10].

We performed a systematic examination of the  $N = 1 \rightarrow N = 2$  and  $N = 2 \rightarrow N = 3$  transitions (where  $N$  is the number of electrons in the dot). These transitions were chosen judiciously since, in addition to being computationally least prohibitive in the EXD method, they exhibit the principal generic features observed in the nonuniversal regime. In particular, for the first transition ( $N = 1 \rightarrow N = 2$ ) no PL was measured, while a phase lapse was found for the second transition. Our calculations reproduce these findings for an appropriate range of dot parameters. From the calculated trends, we predict that: (1) Agreement with the experiment is obtained when the dot parameters (shape and interaction strength) are chosen to be favorable for electron localization (formation of electron molecules enhanced by shape deformation and/or stronger interelectron repulsion). (2) Spin states are important in the selection of transport channels. (3) Excited doorway states play a key role.

*Theory.* The current intensity and the electron-transmission phase through the quantum dot relate to

a quasiparticle-type wave function that can be extracted from the many-body EXD states defined as [6, 11]

$$\varphi_{\text{QP}}(\mathbf{r}) = \langle \Phi_{N-1}^{\text{EXD}} | \psi(\mathbf{r}; \sigma) | \Phi_N^{\text{EXD}} \rangle, \quad (1)$$

where the single-particle operator  $\psi(\mathbf{r}; \sigma)$  annihilates an electron with spin-projection  $\sigma$  at position  $\mathbf{r}$ . For calculating the quasiparticle orbital  $\varphi_{\text{QP}}(\mathbf{r})$ , one uses the relation

$$\psi(\mathbf{r}; \sigma) = \sum_{i=1}^K \phi_i(\mathbf{r}) a_i(\sigma), \quad (2)$$

where  $a_i(\sigma)$  are the annihilation operators in the Fock space and  $\phi_i(\mathbf{r})$  are the single-particle eigenstates of the two-dimensional anisotropic-oscillator potential  $V(x, y) = m^*(\omega_x^2 x^2 + \omega_y^2 y^2)/2$  that confines the electrons in the quantum dot.

The many-body wave functions for a quantum dot with  $N$  electrons are calculated via an exact diagonalization; they are expressed as a linear superposition over Slater determinants  $D$ 's constructed with the spin orbitals  $\phi_i(\mathbf{r})\alpha$  and  $\phi_i(\mathbf{r})\beta$ , with  $\alpha$  ( $\beta$ ) denoting up (down) spins, i.e.,

$$\Phi_N^{\text{EXD}}(S, S_z; k) = \sum_I C_I^N(S, S_z; k) D^N(I; S_z). \quad (3)$$

Observe that, although the Slater determinants conserve only the projection  $S_z$  of the total spin, the EXD wave function in Eq. (3) are after the diagonalization automatically eigenfunctions of the square  $\mathbf{S}^2$  of the total spin, since the many-body Hamiltonian  $\mathcal{H}$  commutes with  $\mathbf{S}^2$ ;  $\mathcal{H} = \sum_{i=1}^N [\mathbf{p}_i^2/(2m^*) + V(x_i, y_i)] + \sum_{i<j} e^2/(\kappa r_{ij})$ .

Two considerations, both derived from characteristics of the electron interferometry experimental setup [2], are key for determining the properties of electron transmission through the tunneling-coupled QD/leads system [6], and in particular for interrogation of the transmission phase [8, 12]: (i) the states of the leads are relatively insensitive to the action of the plunger which serves to vary the number of electrons in the dot [2, 8, 12], and (ii) the experiments in the non-universal regime were performed under conditions where the width of the levels in the QD (due to the coupling to the leads) is much smaller than the level separation in the dot (see p. 531, left column in Ref. [2]), meaning that the QD levels do not overlap. These considerations allow us to focus on the dependence of the transmission phase on the quasiparticle states of the QD as expressed in Eq. (1). In particular, the current intensity through the quantum dot is proportional [6, 11] to the norm (often referred to as the quasiparticle weight)

$$\mathcal{W} = \int |\varphi_{\text{QP}}(\mathbf{r})|^2 d\mathbf{r} \quad (4)$$

of the quasiparticle. Furthermore, the transmission phase  $\theta$  through the quantum dot is given by

$$\theta = \theta_{\text{QP}} - \pi, \quad (5)$$

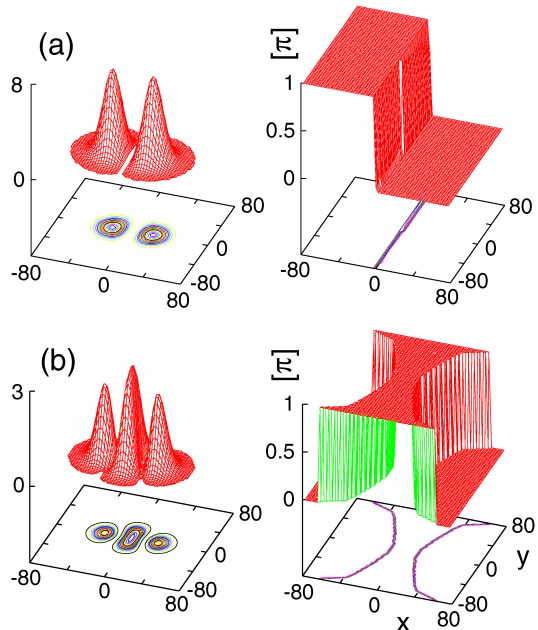


FIG. 1: Quasiparticle wave functions for the  $N = 2 \rightarrow N = 3$  transition in a quantum dot with anisotropy  $\eta = 0.724$ . The initial state is the ground state ( $S = 0, S_z = 0$ ) for  $N = 2$  electrons while the final state is (a) the ground state ( $S = 1/2, S_z = 1/2, E_1 = 20.888$  meV) and (b) the second excited state ( $S = 1/2, S_z = 1/2, E_3 = 23.013$  meV) for  $N = 3$  electrons. (left) quasiparticle amplitudes (modulus square),  $|\varphi_{\text{QP}}(\mathbf{r})|^2$  in units of  $10^{-4}/\text{nm}^2$ ; (right) position-dependent quasiparticle transmission phases. Lengths in nanometers.  $\hbar\omega_x = 4.23$  meV,  $\hbar\omega_y = 5.84$  meV,  $\kappa = 12.50$  (GaAs), and  $m^* = 0.067$  (GaAs).

where the relative quasiparticle phase  $\theta_{\text{QP}} = 0$  if  $\Re[\varphi_{\text{QP}}(\mathbf{r}_L) * \varphi_{\text{QP}}(\mathbf{r}_R)] > 0$  and  $\theta_{\text{QP}} = \pi$  if  $\Re[\varphi_{\text{QP}}(\mathbf{r}_L) * \varphi_{\text{QP}}(\mathbf{r}_R)] < 0$  [12], with  $\mathbf{r}_L$  and  $\mathbf{r}_R$  being the positions specifying the left and right potential barriers that demarcate the quantum dot. When a single Slater determinant (i.e., Hartree-Fock) is used in Eq. (1),  $\varphi_{\text{QP}}(\mathbf{r})$  reduces to a usual single-particle mean-field orbital, and the above considerations involve the parity of that orbital [8].

*Results.* In the following, we study the evolution of the quasiparticle weight  $\mathcal{W}$  and the transmission phase  $\theta$  as a function of the anisotropy parameter  $\eta = \omega_x/\omega_y$  and the strength of correlations expressed via the Wigner parameter  $R_W(\kappa)$  for the two transitions  $N = 1 \rightarrow N = 2$  and  $N = 2 \rightarrow N = 3$ ;  $R_W(\kappa) = (e^2/\kappa l_0)/\hbar\omega_0$  is the ratio between the interelectron Coulomb repulsion and the energy quantum of the harmonic confinement [ $l_0 = \sqrt{\hbar/(m^*\omega_0)}$  is the width of the ground-state Gaussian of the corresponding circular harmonic-oscillator with frequency  $\omega_0 = \sqrt{(\omega_x^2 + \omega_y^2)/2}$ ].

We display in Fig. 1 examples of quasiparticle wave

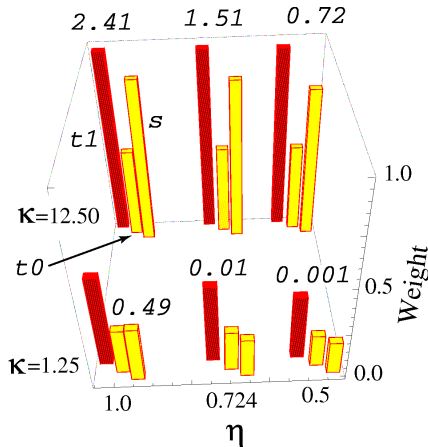


FIG. 2: (Color online) The bar-chart for the quasiparticle of the  $N = 1 \rightarrow N = 2$  transition in a quantum dot as a function of the strength of the interelectron repulsion (stronger for smaller  $\kappa$ ) and the anisotropy  $\eta$ . The heights of the bars indicate the weight  $\mathcal{W}$  [Eq. (4)], while shading denotes the quasiparticle transmission phase [ $\theta_{\text{QP}}$  in Eq. (5)]; dark shade (red) denotes  $\theta_{\text{QP}} = \pi$  (no PL) and gray shade (yellow) denotes  $\theta_{\text{QP}} = 0$  (occurrence of a PL). The bars are arranged in groups of three around each  $(\kappa, \eta)$  point; the right bar corresponds to the singlet ( $s$ ) final state, while the middle and left ones correspond to the final triplet states with spin projection  $S_z = 0$  ( $t0$ ) and  $S_z = 1$  ( $t1$ ), respectively. The numbers above the bars denote the energy difference (in meV) between the ground-state singlet and the excited (degenerate) triplets. The effective mass is  $m^* = 0.067m_e$  (GaAs). For  $\eta = 1.0$ ,  $\hbar\omega_x = 5.0$  meV and  $\hbar\omega_y = 5.0$  meV. For  $\eta = 0.724$ ,  $\hbar\omega_x = 4.23$  meV and  $\hbar\omega_y = 5.84$  meV. For  $\eta = 0.5$ ,  $\hbar\omega_x = 3.137$  meV and  $\hbar\omega_y = 6.274$  meV. Smaller  $\kappa$  and  $\eta$  enhance electron localization in the dot.  $R_W(\kappa = 12.50) = 1.51$  and  $R_W(\kappa = 1.25) = 15.1$ .

functions (amplitude and phase) for the  $N = 2 \rightarrow N = 3$  transition for two different final states (corresponding to the transitions marked 1 and 3 in Fig. 3 below). In Fig. 1(a), the modulus of the quasiparticle wave function exhibits a two-peak structure separated by one node, while the relative transmission phase [difference between the phase values at the exit ( $x = -80$  nm) and entrance ( $x = 80$  nm) points along the  $x$  axis]  $\theta_{\text{QP}} = \pi$ , indicating no phase lapse [see Eq. (5)]. In Fig. 1(b), the modulus of the quasiparticle wave function exhibits a three-peak structure separated by two nodes, while the relative transmission phase  $\theta_{\text{QP}} = 0$ , indicating a PL of  $\pi$  [see Eq. (5)]. The nodal structure reflects the good parity of  $\varphi_{\text{QP}}$ , and it emerges from the many-body EXD calculation (being *a priori* unknown).

We discuss next the  $N = 1 \rightarrow N = 2$  case. Naturally, the initial many-body state is the ground state with one electron (assuming it has a spin up configuration) in the lowest single-particle state in the confining potential  $V(x, y)$ . The final state, however, is not re-

stricted to the singlet ground state [with  $(S = 0, S_z = 0)$ ] of the  $N = 2$  quantum dot. Excited states need to be considered, since an excited “doorway” state may be more efficient in transmitting the current through the quantum dot (i.e., it may have a higher weight). Focussing on the two lowest total energies  $E_k(S, S_z)$ , we are led to consider three final states, i.e., the ground-state singlet ( $S = 0, S_z = 0$ ), and the two excited triplets ( $S = 1, S_z = 0$ ) and ( $S = 1, S_z = 1$ ), which are degenerate at zero magnetic field. The third triplet state ( $S = 1, S_z = -1$ ) has zero weight, since flipping of the direction of the initial spin is not allowed. The calculated EXD results are displayed in Fig. 2.

The heights of the bars in Fig. 2 represent the weight  $\mathcal{W}$ , while the shading (or color online) of each bar denotes the quasiparticle transmission phase, with a dark shade (online red) denoting  $\theta_{\text{QP}} = \pi$  and a gray shade (online yellow) denoting  $\theta_{\text{QP}} = 0$ . Results are presented for two different interelectron interaction strengths (a weaker  $e - e$  repulsion with  $\kappa = 12.50$  and a much stronger  $e - e$  repulsion with  $\kappa = 1.25$ ) and three different dot deformations, i.e.,  $\eta = 1.0$  (circular dot),  $\eta = 0.724$  (moderate anisotropy), and  $\eta = 0.5$  (strong anisotropy).

Inspection of Fig. 2 reveals the following systematic trends: (1) The singlet state and the  $t0$  triplet have in all instances  $\theta_{\text{QP}} = 0$  (with a PL  $\theta = -\pi$ ), while the  $t1$  triplet has  $\theta_{\text{QP}} = \pi$  ( $\theta = 0$ , i.e., no PL). (2) The excited  $t1$  triplet state has always the largest weight  $\mathcal{W}$ , and its relative advantage in  $\mathcal{W}$  compared to the  $t0$  and the  $s$  states increases both for stronger correlations (smaller  $\kappa$ ) and stronger anisotropies (smaller  $\eta$ ). (3) The singlet-triplet energy gap decreases both for smaller  $\kappa$  and smaller  $\eta$ ; that is, for dot parameters that favor formation of Wigner molecules.

Consequently, the  $t1$  triplet state can act as a doorway state for the electron transmission in the case of strong correlations and strong anisotropy. In this case there is no phase lapse ( $\theta = 0$ ), as observed experimentally [2]. We further note the discussion in Ref. [2] which concluded that the experimental observation clearly excluded the ground-state singlet as being the final state of the two electrons. This is in agreement with our theoretical analysis here which concluded that the excited  $t1$  triplet is a realistic candidate for acting as a doorway state.

Next, we discuss the  $N = 2 \rightarrow N = 3$  transition. The initial many-body state is assumed to be the ground state of a QD with two electrons, which is always a singlet [ $(S = 0, S_z = 0)$ ] configuration. As was the case with the  $N = 1 \rightarrow N = 2$  transition, the final state, however, cannot be restricted to the ground state [with  $(S = 1/2, S_z = 1/2)$ ] of the  $N = 3$  system [13]. The possibility that excited states may act as doorway states need to be investigated. Since the transitions to a final ( $S = 3/2, S_z = 3/2$ ) or ( $S = 3/2, S_z = 1/2$ ) state are forbidden (the corresponding  $\mathcal{W} = 0$  due to spin blockade),

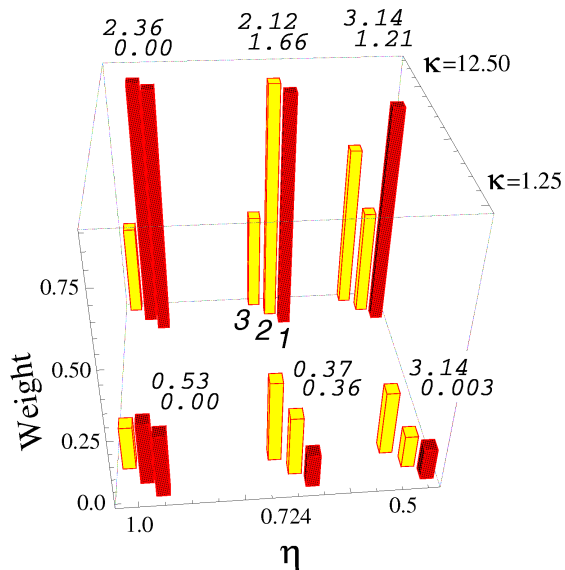


FIG. 3: (color online) The bar-chart for the relevant quasiparticles of the  $N = 2 \rightarrow N = 3$  transition in a quantum dot as a function of the strength of the interelectron repulsion (through the dielectric constant  $\kappa$ ) and the anisotropy  $\eta$ . The heights of the bars indicate the weight  $\mathcal{W}$  [Eq. (4)], with a dark shade (red) denoting  $\theta_{\text{QP}} = \pi$  and a gray shade (yellow) denoting  $\theta_{\text{QP}} = 0$ . In all instances the initial state is the singlet  $[(S = 0, S_z = 0)]$  ground state of the  $N = 2$  dot. The bars are arranged in groups of three around each  $(\kappa, \eta)$  point; the rightmost bar corresponds to the final  $N = 3$  ground state (index 1), while the middle (index 2) and leftmost (index 3) ones correspond to the final  $N = 3$  two lowest excited states with a non-zero weight. All three final states happen to have a  $(S = 1/2, S_z = 1/2)$  magnetic structure. The numbers above the bars denote the energy difference (in meV) between the  $N = 3$  ground-state and the two lowest excited  $(S = 1/2, S_z = 1/2)$  states. The dot parameters are as in Fig. 2.

we are led to consider three final states, i.e., the ground-state with  $(S = 1/2, S_z = 1/2)$  and the two-lowest excited states also with  $(S = 1/2, S_z = 1/2)$  [13]. The calculated EXD results are displayed in Fig. 3, where these three final states are denoted by the indices 1, 2, and 3, respectively. We note that our results apply unaltered for final states with an  $S_z = -1/2$  spin projection.

In Fig. 3, we retain the same conventions as in Fig. 2 concerning the height and shadings (colors online) of the bars. Unlike Fig. 2, the final two-lowest excited states in Fig. 3 are not degenerate, and thus in the latter case we list a pair of energy gaps (in meV) with respect to the final ground state. In the circular case ( $\eta = 1$ ), there are two degenerate final ground states (with total angular momentum  $L = 1$  and  $L = -1$ ) [13], and the smallest meaningful excitation energy gap needs to be taken between the states with indices 1 and 3 (or 2 and 3).

Inspection of Fig. 3 reveals that a transition to the

$N = 3$  ground state (marked 1) will always have  $\theta_{\text{QP}} = \pi$  [corresponding to a dark shade (online red)], and thus it will exhibit no lapse in the transmission phase  $\theta$  [see Eq. (5)], in contrast to the experimental result. It is apparent that transmission through a doorway excited state may become possible for smaller  $\kappa$  (stronger Coulomb repulsion) and smaller  $\eta$  (stronger anisotropy), since as a result (1) the energy gap between the first excited state (index 2) and the ground state diminishes (observe the practically vanishing gap of 0.003 meV for  $\eta = 0.5$  and  $\kappa = 1.25$ ), and (2) the weight  $\mathcal{W}$  of this index-2 final state remains larger than that of the ground state [see the cases with  $(\kappa = 1.25, \eta = 0.724)$  and  $(\kappa = 1.25, \eta = 0.5)$ ]. Transmission through such an index-2 doorway state will lead to a phase lapse ( $\theta = -\pi$ ), since in this case  $\theta_{\text{QP}} = 0$  [gray shade (online yellow)]. Recent experimental measurements [2] have indeed observed a phase lapse in the  $N = 2 \rightarrow N = 3$  transition. As was the case with our analysis of the  $N = 1 \rightarrow N = 2$  transition, this observation of a phase lapse and our EXD analysis of the  $N = 2 \rightarrow N = 3$  transition suggest that the experimental quantum dots were strongly deformed and exhibited rather strong interelectron correlations.

*Conclusions.* In summary, focusing on the mesoscopic regime of electron interferometry, and using a computational transport theory involving exact diagonalization of the many-body quantum dot Hamiltonian, we have shown for the first two transitions, (a)  $N = 1 \rightarrow N = 2$  and (b)  $N = 2 \rightarrow N = 3$ , nonuniversal behavior of the transmission phases with no phase lapse for (a) and a phase lapse of  $\pi$  for (b), in agreement with the experiment [2]. These results were obtained for a range of dot parameters characterized by shape anisotropy and strong  $e - e$  repulsion, with both favoring electron localization and formation of Wigner molecules [5, 14]. Additionally, our analysis of the quasiparticle wavefunction [Eq. (1)] highlights the dependence of the phase-lapse behavior on the spin configurations of the initial and final states, and the importance of excited doorway states as favored transmission channels. Electron interferometric measurements on dots with controlled shapes, and extension of our analysis to a larger number of electrons, including the transition to the universal regime, remain future challenges.

Work supported by the US D.O.E. (Grant No. FG05-86ER45234). Calculations were done at NERSC, Berkeley, CA. We thank S.A. Gurvitz for bringing Ref. [12] to our attention.

- 
- [1] R. Schuster *et al.*, Nature **385**, 417 (1997).
  - [2] M. Avinun-Kalish *et al.*, Nature **436**, 529 (2005).
  - [3] See articles in *Focus on Interference in Mesoscopic Systems*, New J. Phys. **9** (May 2007).
  - [4] C. Karrasch *et al.*, Phys. Rev. Lett. **98**, 186802 (2007).

- [5] C. Yannouleas and U. Landman, Rep. Prog. Phys. **70**, 2067 (2007), and references therein.
- [6] J. Bardeen, Phys. Rev. Lett. **6**, 57 (1961).
- [7] A treatment of the scattering problem and Fano-type resonance profiles, involving scattering states in the leads and many-body states in a one-dimensional dot, is described in F. Buscemi *et al.*, Phys. Rev. B **76**, 195317 (2007)].
- [8] G. Hackenbroich and H.A. Weidenmüller, Phys. Rev. Lett. **76**, 110 (1996).
- [9] G. Hackenbroich, Phys. Rep. **343**, 464 (2001).
- [10] C. Ellenberger *et al.*, Phys. Rev. Lett. **96**, 126806 (2006).
- [11] See section 8.2.1. in J. Callaway, *Quantum Theory of the Solid State* (Academic, New York, 1991) 2<sup>nd</sup> edition.
- [12] S.A. Gurvitz, arXiv:0704.1260v1 (2007).
- [13] (a) For the EXD spin configurations of an  $N = 3$  circular QD, see S.A. Mikhailov, Phys. Rev. B **65**, 115312 (2002). For an anisotropic QD, see Y. Li *et al.*, Phys. Rev. B **76**, 245310 (2007). (b) See also R. Pauncz, *The Construction of Spin Eigenfunctions: An Exercise Book* (Kluwer/Plenum, New York, 2000).
- [14] For  $N = 2$  see Ref. [10], and for  $N = 3$  see Ref. [13(a)].